AN IMPROVED HIGH-SPECTRAL RESOLUTION WATER FILLED IMPEDANCE TUBE MEASUREMENT METHOD FOR MARINE SEDIMENT STUDIES

L J North National Oceanography Centre Southampton
A I Best National Oceanography Centre Southampton

1 INTRODUCTION

The acoustic properties of water saturated seafloor sediments have been well documented in recent decades and are reasonably well understood. However, the same cannot be said for seafloor sediments containing free gas (gassy sediments), and even less is known about the acoustic properties of methane hydrate-bearing sediments. Seafloor methane hydrates are ice-like compounds found in deep water continental margin sediments around the world. They are increasingly being viewed as important for their possible impacts on climate change, their geohazard potential and as a source of natural gas for energy. A major challenge is to quantify the amount of methane hydrate present beneath the seafloor, and hence estimate the amount of greenhouse gas (methane) that could be released into the water column during warming of the oceans, such as in the present day Arctic. This requires improved geophysical remote sensing including improved seismo-acoustic methods.

Previous studies have shown that P- and S-wave velocities and attenuations can increase with hydrate content in sands[1,2,3], but the picture is complicated by variations in hydrate morphology influenced by sediment type. For example, fine disseminated hydrate can form in sands, but hydrate tends to form nodules, sheets or lenses in muds[4]. To better understand the effects of hydrate content and morphology, and frequency dependence, on velocity and attenuation, we have developed a novel acoustic impedance tube instrument that allows the creation of methane hydrate in sediment samples in the laboratory and acoustic velocity and attenuation measurements in the frequency range 1 – 10 kHz.

One aspect of sediments hosting methane hydrate is that we expect both free gas and hydrate to co-exist. These natural composites of gas bubbles, solid hydrate and sediment could display strong velocity and attenuation dispersion in a similar manner to observations and theoretical predictions for gassy sediments[5,6]. Previous work by McCann et al.[7] demonstrated the use of a water filled impedance tube to determine the average velocity and attenuation of sediment samples over a frequency range of 2 - 8 KHz. In this paper we describe a new acoustic signal processing method that allows the frequency dependent velocity and attenuation of sediment samples to be extracted from impedance tube measurements, needed for hydrate studies. Preliminary results of the frequency dependent complex velocity of jacketed nylon from 1 to 10 kHz are in good agreement with finite element numerical (COMSOL) simulations and analytical model predictions.

2 INSTRUMENTATION

Acoustic impedance tubes are a mature technology commonly used to determine the acoustic properties of materials in a variety of host mediums including air and water[8,9]. The National Oceanography Centre (NOC) Southampton water filled acoustic impedance tube is 4.5 meters long with a 70 mm bore and 252 mm outside diameter (figure 1).

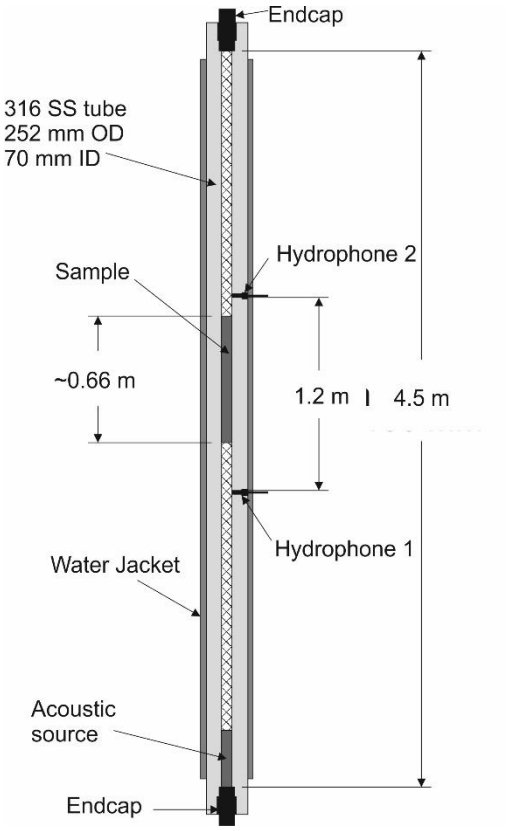

Figure 1, Schematic of the NOC Southampton water filled impedance tube.

Cylindrical sediment or rock samples up to 1m long are positioned in the tube between two hydrophones that are located in the wall of the tube. An acoustic source, located inside the base of the tube, is used to project sound at the sample. Measurements of the sound transmitted through, and reflected by, the sample are then used to determine sound velocity and attenuation in the sample. We use an acoustic source developed at the NOC due to a lack of commercially available devices. The source is compact (68 mm OD, 200 mm long), intrinsically pressure equalised and capable of nearly a decade of usable bandwidth from 1 to 10 kHz with a sensitivity of approximately 160 dB 1V/uPa, as measured in the impedance tube (figure 2). The source transducer is driven by a low voltage, low output impedance amplifier based upon the Texas instruments LM3886 IC, which in-turn is driven by a Keysight tech. programmable arbitrary function generator. We use a 2 second long logarithmically swept chirp waveform to increase the signal to noise ratio (SNR) of our measurements.

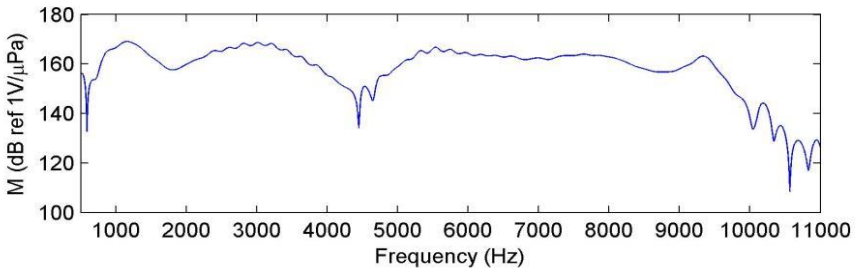

Figure 2, In-tube frequency response of the impedance tube acoustic source

The hydrophones used are Neptune Sonar Ltd. type B-200 with a maximum working pressure of 7 MPa. We are currently developing intrinsically pressure compensated hydrophones to fully exploit the high pressure capability of the impedance tube (max. 60 MPa or ~8700 psi).

The signals from the hydrophones are conditioned by a Brüel & Kjær preamplifier and recorded using a LeCroy oscilloscope. The SNR we obtain we obtain for the complete system is > 60 dB from 1 to 10 kHz. The tube is surrounded by a water jacket enabling a controlled operational temperature range of 0 – 50 ˚C. Pressure is monitored using a Keller piezo resistive transducer with an accuracy of 0.04 MPa. And temperature is controlled via a custom heater/chiller unit with a thermocouple inside the pulse tube giving temperature accuracy of ±0.5 ˚C.

3 DATA INVERSION

3.1 Inversion Method

Our data inversion method is based upon the iterative minimisation of least-squares misfit between a 1D frequency domain transmission line forward model of the impedance tube and measurements. This method is analogous to those used for the determination of electromagnetic properties at microwave frequencies[10]. It was apparent from initial calibration attempts that the complex transfer functions of our hydrophones were sensitive not only to pressure and temperature but also the specific port in which the hydrophone was inserted. Therefore, typical hydrophone switching[11] and water/air interface[9] calibration methods could not be used. Instead, we developed a water reference technique, whereby the complex ratios between measurements made with and without the sample are used to determine the velocity and attenuation of both the sample and the host medium, in our case water. The 1D transmission line forward model of the tube assumes plane wave propagation, which, given the ratio of tube bore to tube outside diameter and material choice (316 SS), is valid[9]. We begin our development of the 1D forward model by assuming the acoustic pressure field within the pulse tube has time dependence $e^{j\omega t}$, we then define the transmission coefficient, γ, as

$$\gamma = \exp(i\frac{w}{c}d) \quad \text{Eqn 1}$$

where ω is angular frequency, c is complex velocity in the medium and d is propagation distance. We define the reflection coefficient, Γ between the sample and host medium by

$$\Gamma = \frac{z_w - z_s}{z_w + z_s} \quad \text{Eqn 2}$$

where z_s and z_w are the acoustic impedance of the sample and surrounding water respectively. The acoustic impedance, z , of a medium is given by

$$z = \rho c \quad \text{Eqn 3}$$

Where ρ and c are the density of, and speed of sound in the medium respectively. The total reflection signal, P_r , from the sample, measured by hydrophone 1 including the incident pressure field and excluding any reflections from the endcaps of the impedance tube is given by

$$P_r = P_{inc}H_1 + \gamma_{w1}^2 P_{inc}H_1\left[\Gamma - \Gamma\gamma_s^2\left(1-\Gamma^2\right)\left(1+r+r^2+r^3+\ldots r^n\right)\right] \quad \text{Eqn 4}$$

where

$$r = \Gamma^2\gamma_s^2 \quad \text{Eqn 5}$$

and P_{inc} is the incident pressure field, H_1 is the complex transfer function of hydrophone 1, γ_{w1} is the propagation coefficient in water between hydrophone 1 and the front bounding surface of the sample and γ_s is the propagation coefficient within the sample. The total transmitted signal recorded by hydrophone 2, P_t , measured at the bounding surface of the sample, including all partial reflections within the sample, is given by

$$P_t = \gamma_{w1}\gamma_{w3}P_{inc}H_2\left[\gamma_s\left(1-\Gamma^2\right)\left(1+r+r^2+r^3+\ldots r^n\right)\right] \quad \text{Eqn 6}$$

where H_2 is the complex transfer function of hydrophone 2 and γ_{w3} is the propagation coefficient in water between the rear bounding surface of the sample and hydrophone 2. In the limit where $n \to \infty$ (including all partial reflections within the sample) equations 4 and 6 converge to

$$P_r = P_{inc}H_1 + \gamma_{w1}^2 P_{inc}H_1 \frac{\Gamma\left(1-\gamma_s^2\right)}{1-\gamma_s^2\Gamma^2} \quad \text{Eqn 7}$$

and

$$P_t = \gamma_{w1}\gamma_{w3}P_{inc}H_2 \frac{\gamma_s\left(1-\Gamma^2\right)}{1-\gamma_s^2\Gamma^2} \quad \text{Eqn 8}$$

Equations 4 and 6 – 9 include the terms γ_{w1} and γ_{w3} because in practice sample length is chosen to maintain a distance of 100 – 400 mm between the hydrophones and bounding surfaces of the sample. These gaps are desirable because the wavefront is non-planar close to the bounding surfaces of the sample which is a result of the sample diameter being 1 or 2 mm less than the impedance tube bore for mechanical clearance. The transmission line model of the water reference signals from hydrophones 1 and 2 without the sample present is given by equations 9 and 10 respectively.

$$P_{w1} = P_{inc}H_1 \quad \text{Eqn 9}$$

$$P_{w2} = \gamma_{w1}\gamma_{w2}\gamma_{w3}P_{inc}H_2 \quad \text{Eqn 10}$$

The term γ_{w3} in equation 10 represents sound propagation in water over the length of the sample. The complex ratio of the reflected pressure field R, for a sample filled and empty, water filled, impedance tube is given by;

$$R = \frac{P_r}{P_{w1}} = 1 + \gamma_{w1}^2\left[\Gamma - \Gamma\gamma_s^2\left(1-\Gamma^2\right)\left(1+r+r^2+r^3+\ldots r^n\right)\right] \quad \text{Eqn 11}$$

The complex ratio of the reflected pressure field T, for a sample filled and empty, water filled, impedance tube is given by;

$$T = \frac{P_t}{P_{w2}} = \frac{1}{\gamma_{w2}}\left[\gamma_s\left(1-\Gamma^2\right)\left(1+r+r^2+r^3+\ldots r^n\right)\right] \quad \text{Eqn 12}$$

The complex sound velocity within the sample and in the surrounding host water is then found by minimising the least squares misfit between the forward model value of R and T given by equations 11 and 12 and the measured values. While the minimisation is reasonably robust we find that constraining sample water loss to be positive improves consistency of results and makes the process less sensitive to initial starting parameters.

The data inversion method described above finds the Stoneley/Scholte wave velocity of the sample and surrounding host water, which must then correct to find bulk velocity. We show later how this conversion may be performed by comparison to analytic[12] and finite element models.

3.2 Processing Workflow

The processing workflow is shown in figure 3. The first processing operation is transformation of the recorded time domain signals to the frequency domain. A chirp anti-filter is then applied to retrieve the impulse response of the system. Because the impedance tube is of finite length, reflections from the endcaps are superimposed on the full series of partial reflections within the sample. Hence the endcap reflections, which are not included in the transmission line forward model (equations 11 and 12), must be excluded by time-domain gating. To do this effectively the time domain impulse response must be temporally compact, thus we apply a Chebyshev type sharpening filter in the frequency domain. The signals are then transformed back to the time domain and a suitable interval to apply time domain gating is identified so as to exclude endcap reflections. A Tukey type window is used to gate the time domain signal. The result of the chirp anti-filter, sharpening filter and time domain gating processes is shown in figure 4. Depending upon sample length and acoustic loss the time domain series described by equations may not tend to zero thus equations 11 and 12 must be appropriately truncated to include the correct number of partial reflections.

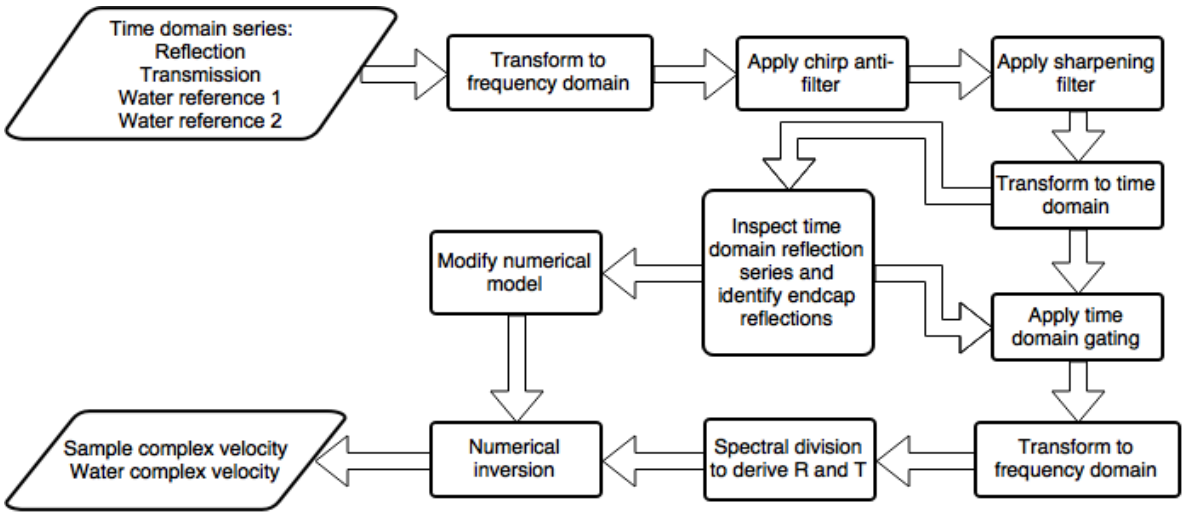

Figure 3, Processing workflow

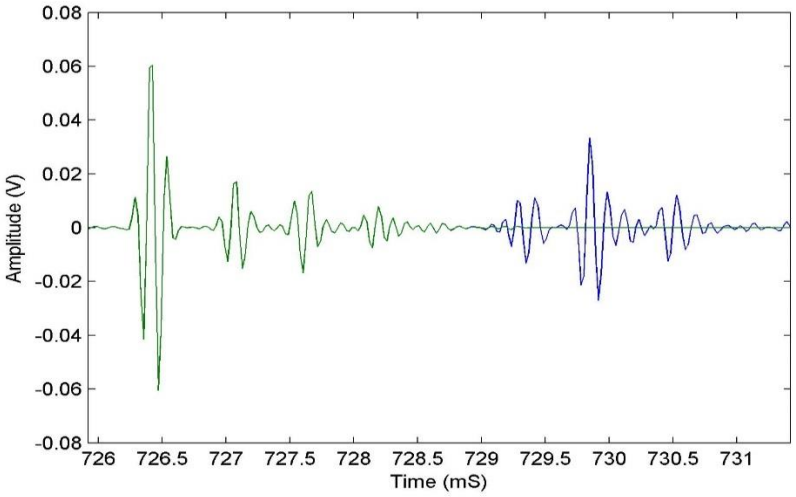

Figure 4, An example of a typical impulse reflection response of a nylon sample after application of a Chebyshev sharpening filter. The initial incident impulse can be seen followed by 3 partial reflections from within the sample followed by a train of reflections from the endcaps. The green portion of signal indicates the time domain gated section used in subsequent processing stages.

4 RESULTS

4.1 Method Validation

We first validated the efficacy of the data inversion method by processing synthetic results generated using COMSOL finite element modelling software (FE model 1 in figure 5). We modelled both the water and water/sampled filled impedance tube in the time domain. The FE sample model was a 600 mm long cylinder with a diameter of 35 mm, thus the sample completely filled the bore of the tube without a gap around the perimeter. The sample model had a compressional wave velocity of 2700 ms^{-1} and density of 1140 kgm^{-3} similar to that of the nylon 66 used in our subsequent experiments. We assumed quasi-plane compressional wave propagation in the tube and neglect shear wave components. The host water compressional wave velocity used in the model was specified as 1438 ms^{-1}. This velocity was calculated using the model given by Belogolskii et al. [13] for the temperature, 7°C, and pressure, 7 MPa, of our subsequent experiments. We set the loss for both the sample and host water to zero for this initial synthetic model. Our results are presented in figure 5 together with a summary of mean velocity and standard deviation, σ, in table 1. The FE model 1 results show a mean sample velocity of 2544 ms^{-1} with a standard deviation of 15 ms^{-1}. This is in good agreement with the velocity of 2551 ms^{-1} analytic model predicted by the analytic model given by Del Grosso[12]. Sample loss is almost zero from 2 – 10 kHz, although some small (< 1dB) peaks are evident at specific frequencies. The analytic water Scholte wave velocity prediction (1419 ms^{-1}) is also in excellent agreement with our FE validation result (1423 ms^{-1}).

4.2 Measurement Results

Our measurement results were obtained using a 634 mm long 60 mm diameter Nylon 66 sample with a 4 mm thick butyl rubber jacket resulting in an overall sample diameter 68 mm. This replicates the likely sample jacket configuration we will use for sediment samples. The results were obtained at a temperature of 7˚C and a pressure of 7.00 MPa (~ 1015 psi). We performed 3 sets of independent measurements to assess measurement precision. Our results show a consistent velocity for the sample of 2284 - 2285 ms^{-1} with a standard deviation of less than 24 ms^{-1} which is significantly less than that predicted by the analytic model (2544 ms^{-1}) . To investigate this discrepancy inverted FE model datasets where the sample diameter was reduced incrementally. We found that while the apparent Stoneley wave velocity fell significantly with decreasing sample diameter, with a model sample diameter of 66 mm giving a good match to our measured results. While our jacketed sample has an overall diameter of 68 mm, the outer 4 mm is the rubber jacket, thus the optimal 66 mm model (FE model 2) represents an effective equivalent diameter for the composite rubber/nylon jacketed sample. The velocity we obtained for the host water is between 1411 ms^{-1} and 1420 ms^{-1} with a standard deviation of less than 9 ms^{-1} in agreement with the predicted value of 1419 ms^{-1}. Loss in the sample shows an increase from approximately 1 dBm^{-1} at 2kHz to 5 dBm^{-1} at 10 kHz. While the FE models showed sample velocity was sensitive to sample diameter, loss remained almost unchanged. To model the observed loss in our samples we introduced viscous Stokes type attenuation in FE model 2 and found that both the FE model and the analytic model of attenuation agreed well with the observed loss for nylon 66 given a bulk viscosity of $8x10^{3}$ Pa·s.

5 CONCLUSIONS

We have demonstrated a new method to extract the frequency-dependent velocity and attenuation of samples at high pressure. Our method accurately inverts synthetic FE data to give results that are in excellent agreement with analytic models. Notwithstanding our small sample size our initial results indicate a precision (1 standard deviation) of approximately 1 % for velocity and 1 dBm^{-1} for attenuation for our system. The accuracy of our results can be gauged by the degree of agreement between our measured and synthetic results. However, further measurements will be required to validate these initial observations.

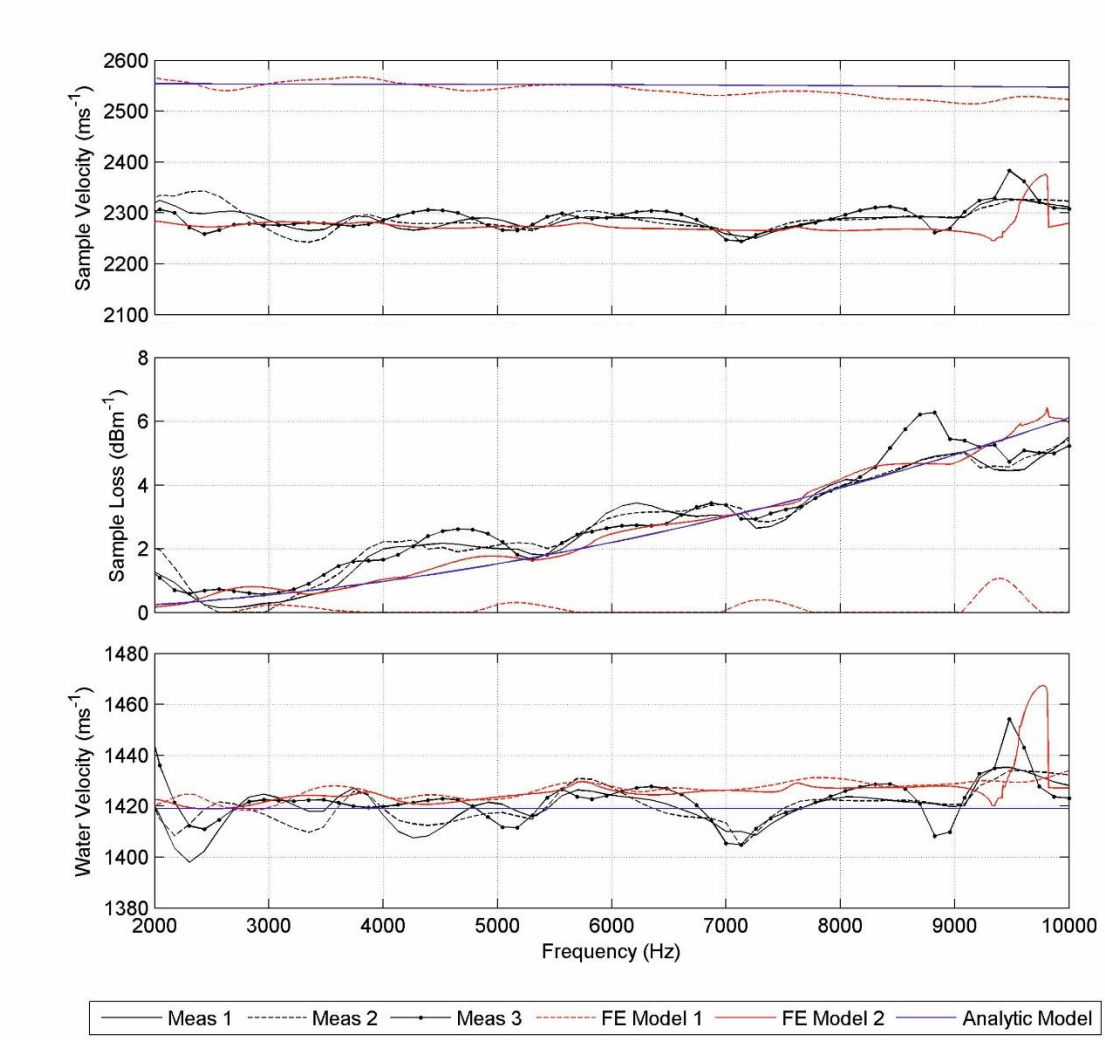

Figure 5, Velocity and attenuation results for samples and models.

Table 1, Mean velocity and standard deviation for measurements and models.

Sample name	**Mean Sample Velocity (ms^{-1})**	**σ sample (ms^{-1})**	**Mean Water Velocity (ms^{-1})**	**σ water (ms^{-1})**
Jacket meas. 1	2284	18	1411	8
Jacket meas. 2	2285	24	1412	7
Jacket meas. 3	2284	24	1420	9
FE model 1	2544	18	1423	4
FE model 2	2284	15	1419	7
Analytic Model	2551		1419	

6 REFERENCES

1. Best, A.I., et al., The effect of methane hydrate morphology and water saturation on seismic wave attenuation in sand under shallow sub-seafloor conditions. Earth and Planetary Science Letters, 368(78-87. (2013)
2. Guerin, G. and D. Goldberg, Sonic waveform attenuation in gas hydrate-bearing sediments from the Mallik 2L-38 research well, Mackenzie Delta, Canada. Journal of Geophysical Research-Solid Earth, 107(B5) (2002)
3. Priest, J.A. and A.I. Best, A laboratory investigation into the seismic velocities of methane gas hydrate-bearing sand. Journal of Geophysical Research-Part B-Solid Earth, 110(B4) 13 pp.-13 pp. (2005)
4. Riedel, M., E.C. Willoughby, and S. Chopra, Gas Hydrates - Geophysical Exploration Techniques and Methods. Geophysical Characterization of Gas Hydrates, 14) 1-22. (2010)
5. Anderson, A.L. and L.D. Hampton, ACOUSTICS OF GAS-BEARING SEDIMENTS .1. BACKGROUND. Journal of the Acoustical Society of America, 67(6) 1865-1889. (1980)
6. Leighton, T.G., Theory for acoustic propagation in marine sediment containing gas bubbles which may pulsate in a non-stationary nonlinear manner. Geophysical Research Letters, 34(17) (2007)
7. McCann, C., J. Sothcott, and A.I. Best, A new laboratory technique for determining the compressional wave properties of marine sediments at sonic frequencies and in situ pressures. Geophysical Prospecting, 62(1) 97-116. (2014)
8. Sabin, G.A., Acoustic-Impedance Measurements at High Hydrostatic Pressures. The Journal of the Acoustical Society of America, 40(6) 1345-1353. (1966)
9. Wilson, P.S., R.A. Roy, and W.M. Carey, An improved water-filled impedance tube. Journal of the Acoustical Society of America, 113(6) 3245-3252. (2003)
10. Bakerjarvis, J., E.J. Vanzura, and W.A. Kissick, IMPROVED TECHNIQUE FOR DETERMINING COMPLEX PERMITTIVITY WITH THE TRANSMISSION REFLECTION METHOD. Ieee Transactions on Microwave Theory and Techniques, 38(8) 1096-1103. (1990)
11. Chung, J.Y. and D.A. Blaser, TRANSFER-FUNCTION METHOD OF MEASURING IN-DUCT ACOUSTIC PROPERTIES .1. THEORY. Journal of the Acoustical Society of America, 68(3) 907-913. (1980)
12. Delgross.Va, ANALYSIS OF MULTIMODE ACOUSTIC PROPAGATION IN LIQUID CYLINDERS WITH REALISTIC BOUNDARY CONDITIONS - APPLICATION TO SOUND SPEED AND ABSORPTION MEASUREMENTS. Acustica, 24(6) 299-&. (1971)
13. Belogol'skii, V.A., et al., Pressure dependence of the sound velocity in distilled water. Measurement Techniques, 42(4) 406-413. (1999)